Appl Nanosci (2014) 4:305–313
DOI 10.1007/s13204-013-0196-y

ORIGINAL ARTICLE

Synthesis, characterization and application of TiO_2 nanopowders as special paper coating pigment

Samya El-Sherbiny · Fatma Morsy · Marwa Samir · Osama A. Fouad

Received: 13 December 2012 / Accepted: 16 January 2013 / Published online: 2 March 2013

Abstract TiO_2 nanopigments in two pure crystallographic forms (anatase and rutile) have been synthesized successfully by two methods; hydrothermal and hydrolysis. The produced pigments from the two methods were investigated physicochemically by several analyses tools. Then they were applied in paper coating mixtures and their influence on coated paper properties was systematically investigated. XRD and FTIR investigations showed that the prepared pigments using hydrothermal method at 100 and 120 °C were a mixture of anatase and brookite and pure anatase, respectively, whereas hydrolysis method produced pure rutile phase pigment. TEM investigation showed that the crystallite size of anatase, mixture of anatase and brookite and rutile samples are 6.2, 11.7, and 9.2 nm, respectively. BET studies proved that anatase pigment has 140.74 m^2/g, 0.237 cc/g and 18.33 Å, whereas rutile has 60.621 m^2/g, 0.122 cc/g and 14.669 Å, surface area, pore volume and pore diameter, respectively. UV–Vis absorption and PL emission characteristics of the prepared pigments showed that the energy gaps for anatase, mixture of anatase and brookite and rutile are 3.36, 3.30 and 3.37 eV, respectively. The addition of the prepared nanopigments in conjugation with clay in coating mixture increased both brightness and opacity of the coated papers. The greatest effect was obtained upon using rutile nanopigment. Also there was a significant decrease in coated paper roughness while the air permeance started to decrease then increased at 50 % addition levels. In all coated paper, rutile pigment showed the highest enhancement effect on coated paper properties.

Keywords TiO_2 nanopigments · Paper coating · XRD · SEM · Optical properties

S. El-Sherbiny (✉) · F. Morsy · M. Samir
Paper and Printing Laboratory, Chemistry Department, Faculty of Science, Helwan University, Helwan, Egypt
e-mail: samya.elsherbiny@gmail.com

O. A. Fouad (✉)
Nanostructured Materials and Nanotechnology Laboratory, Advanced Materials Department, Central Metallurgical Research and Development Institute (CMRDI), P.O. Box 87, Helwan, Cairo 11421, Egypt
e-mail: oafouad@yahoo.com

Introduction

The advancing technologies of printing and packaging have placed greater demands on the surface of the paper sheet. To meet the more stringent requirements, many papers are coated with suitable pigment-rich formulation to provide gloss, smoothness, color, print detail, and brilliance by filling in the void area on the surface of the paper sheet and covering the highest sitting fibers on the base paper surface (Smook 1997). The coating mixtures are highly concentrated water-based suspensions containing, among other additives, inorganic pigments, binder thickeners and other additives.

Pigment is the most abundant component in the coating, so pigment is naturally the most important factor affecting the properties of the coating materials (Gullichsen et al. 2000). Pigments are used as a blend of different sizes and shapes of various pigment materials. Various specialty pigments with higher cost are often introduced in small amounts to optimize the coating properties (Ninness et al. 2003).

One of the most commonly used paper coating pigments are clays. Clays are hydrous aluminum silicates combined with many other mineral species. Kaolin as one kind of clay minerals have been used as the leading white pigment

in paper fillers, paper coating and other different applications such as ceramics, paint, cracking catalyst, cements, waste water treatment, and pharmaceutical industries. Although Kaolin is a commercially available and low-cost paper coating pigment, the need for special paper with special optical characteristics has limited its use in paper coating. Kaolin has comparable whiteness, but lower light scattering index (83.5 m^2/kg) than that of the TiO_2 micropowder pigment (254.7 m^2/kg), nowadays used commonly (Murray and Elzea 2005).

Recently, titanium dioxide nanopowder has received much interest. This is due to its use in various applications such as cosmetics, paper and medical devices coating and gas sensors (Deorsola et al. 2008; Kobayashi et al. 2008; Wang et al. 2008). Several papermaking trends necessitate more use of TiO_2 including reduction in basis weight and the increasing use of cheap, discolored fibers. Also, because TiO_2 is used in a large variety of products, its global demand growth is increasing rapidly along with its exceptionally high price. It has variety of advantages such as high surface tension, specific surface area, magnetic property, lower melting point, good thermal conductivity and environmentally friendly (John 2006; Qiong et al. 2008). TiO_2 is a polymorphic compound that exists mainly in three crystallographic phases: anatase, rutile and brookite. They are different in their synthesis and properties among which rutile and anatase are the most commonly synthesized phases owing to their good thermodynamic characteristics and physical properties. Rutile phase has a more compact tetragonal crystal structure than anatase pigment, which might be the reason for its higher refractive index (2.903). In photocatalysis research, where an external UV source is used, anatase titania is usually considered to be more active than rutile but rutile titania possesses better photoabsorption property in visible light wavelength range. In addition, rutile titania exhibits an excellent refractive index, high dielectric constant, higher hiding power and superior chemical stability (Bok et al. 2007; Yamamoto et al. 2009 and Jiaguo et al. 2003).

Titanium dioxide nanopowder was prepared by different methods such as combustion (Deorsola and Vallauri 2008), solvent evaporation (Fumin et al. 2007), hydrothermal (Kobayashi et al. 2008; Yamamoto et al. 2009; Inagaki et al. 2001; Kumar et al. 2009) and hydrolysis (Mahshid et al. 2007; Zhang et al. 2009; Jun et al. 2007; Dahlvik et al. 2000). Its particle size could be precisely controlled in industrial applications to maximize its reflectance. It is used in paper coating to increase both brightness and opacity. Because of the shortness of Ti resource and its relatively high value, low-cost synthesis techniques for TiO_2 pigment have been investigated. Moreover, phase control in TiO_2 synthesis is an interest for many research groups.

Here we report on the preparation of titanium dioxide nanopigments with various morphologies by two methods namely; hydrothermal and hydrolysis at room temperature. A comparison between the characteristics of the produced titanium dioxide nanopigments from both routes is explored. Moreover, the use of the produced titanium dioxide nanostructures as a pigment in paper coating is also investigated.

Experimental

Materials

The materials used in the present study to prepare nano titanium dioxide particles were, Titanium (IV) isopropoxide ($C_{12}H_{28}O_4Ti$, TTIP, 97 %, Aldrich), Tetrabutyl-orthotitanate ($C_{16}H_{36}O_4Ti$, 97 %, Fluka), as titanium precursor. Hydrochloric acid (HCl, assay 30 %, Sic) was used as a hydrolyzing agent. Ethyl alcohol (C_2H_5OH, 95 %, Adwic) was used as washing, drying and nonaqueous media agent. Urea ($NH_2.CO.NH_2$, 99 %, Adwic) was also used as a structure directing agent. All reagents were of chemical grade and were used as received without any further treatment.

Acrylic copolymer latex (Acronal S801, BASF), clay pigment (EMAK company) and sodium hexametaphosphate dispersant (99 %, Fine chemical company) were used for preparation of coating mixture.

Preparation of titanium dioxide nanopigments

Titanium dioxide nanopowders were prepared using two methods namely: (i) hydrothermal method and (ii) hydrolysis method at room temperature.

In the case of hydrothermal method, a clear solution was obtained through addition of 0.2 molar of titanium isopropoxide dropwise into a mixture of 0.79 molar ethanol and 0.58 molar concentrated hydrochloric acid under magnetic stirring. Then the above mixture was diluted by adding distilled water. After stirring for half an hour, the mixture was transferred into Teflon-lined stainless steel autoclave. The autoclave was sealed and subjected to heat treatment at a temperature ranges from 100 to 140 °C for 24 h.

In the case of hydrolysis method at room temperature, the typical experimental procedure was as follows: 0.02 molar of tetrabutyl orthotitanate [$Ti(OC_4H_9)_4$] was dissolved in 1.59 molar ethanol. After stirring for half an hour, the resulting solution was added dropwise into a 100 ml of 0.25 molar urea in an ice bathed diluted hydrochloric acid aqueous solution under vigorous stirring to form a misty mixture. After further stirring for 4 h, the mixture was allowed to stand at room temperature for almost 2 weeks.

The obtained products from the two methods were washed several times with distilled water and then were

centrifuged and kept in the suspension status for further paper coating applications.

Application of the prepared nano TiO_2 pigment in paper coating

Preparation of coatings

The basic coating formula used in this study was consisted of 100 pph clay pigment, 15 pph binder and 0.3 parts of dispersant (pph = part per 100 parts of dry pigment). This sample was used as a reference sample. The prepared titanium dioxide nanopigments were used at 30 and 50 pph in conjugation with clay.

The coating mixtures were prepared in three steps. First, the pigment was dispersed in water in a high shear mixer for 20 min at 50 % solids content with sodium hexametaphosphate dispersant. Second, the pre-dispersed binder was gradually added, over a 5-min period to the pigment slurry; for this step the impeller speed was reduced to a moderate speed. Finally, water was added to obtain the desired solids content. The pH was adjusted to 8.5 by adding few drops of 1 M sodium hydroxide solution to the coating mixture.

Preparation of coated paper samples

A K-bar semiautomatic coater (model NOS k101, R&K print coat instruments Ltd, United Kingdom) was used for applying the coating mixtures. A wire-wound coating bar was chosen to give a 6-μm thick wet film. Paper samples to be coated were cut to overall dimensions of 200 × 300 mm using strip cutter, and were coated under standard conditions of temperature and humidity 23 ± 1 °C and 50 ± 2 % RH according to ISO 187.

Characterization of the prepared pigments and coated paper samples

The crystal structure, phase identification, purity, crystallinity and crystallite size for the prepared pigments were done by X-ray diffraction (XRD; Bruker axs D8, Germany) using Cu-Kα ($\lambda = 1.5406$ Å) radiation and secondary monochromator in the range 2θ from 10 to 80. Crystallite size is automatically calculated from XRD data. Bonding structures were analyzed using Fourier transform infrared spectrometer (FTIR-460*plus*, JASCO model 6100, Japan). The pigment samples were ground with KBr (1:100 ratios) and mounted as a tablet to the sample holder in the cavity of the spectrometer. The spectra were recorded on a single-beam spectrometer with a resolution of 4 cm^{-1} at room temperature in the range 400–4,000 cm^{-1}. The specific surface area (SBET), pore volume and pore size distribution of the prepared samples were determined by N_2 adsorption desorption technique using BET surface area analyzer (Auto Sorp-1-Mp surface area 2008). The samples were degassed at 250 °C for 3 h before analysis, and the N_2 isotherms were obtained at 196 °C. The morphological structure of the pigment samples was investigated using scanning electron microscopy (SEM, Jeol-JSM-5410, Japan) and high resolution analytical transmission electron microscopy (TEM, Jeol, JEM-2010, Japan) operating at a maximum of 200 kV. The optical properties of the prepared pigment materials were measured in air at room temperature. The UV–visible absorption spectra were recorded in the wavelength range of 200–800 nm using a spectrophotometer (UV–Vis, JASCO V-570, Japan). Photoluminescence (PL) spectra were collected in the scan range from 300 to 900 nm using a luminescence spectrometer (RF-5301) with xenon lamp as the excitation source. UV–Vis and PL spectra were measured using a quartz cuvette (Q10) of 1 cm path length. Ultrasonically dispersed TiO_2 nanopowders in ethanol solution were introduced into the cuvette and exposed to source light. As the UV light could be absorbed pretty quickly so the sample suspensions should be very dilute.

The properties of coated papers including the prepared nanopigments were evaluated using standard tests for physical and optical properties. The surface microstructure is observed by scanning electron microscope (XL30, Philips). Gloss is a property that refers to the quality of luster, or ability of the surface to show an image. A micro glossmeter was used, at an angle of 75°, to measure the gloss of coated paper samples. Paper brightness is referred to the overall reflectivity i.e., visual efficiency of the paper. The measurements were conducted on brightness and colorimeter instrument (model 68-59-00-002, Buchel-B.V, Netherlands) according to standard method of ISO 2470-1 (2009). Opacity was also measured using the same instrument according to ISO 2471 (2008). Paper roughness is defined as the measurement of the extent to which the surface of the paper deviates from plane; it is measured by the rate of flow between the paper sample and another standard surface in contact with it. It was measured in ml/min by roughness tester (Bendtsen; model K531, Messmer Bunchel) according to ISO 8791-2 standard. Air permeance is the mean flow of air through unit area under unit air-pressure difference in unit time under specified conditions and it was measured in ml/min by the roughness tester according to ISO 5636 standard.

Results and discussion

Characterization of titanium dioxide nanopigments

Crystal and bond structures

Figure 1 shows the XRD patterns of the prepared nano titanium oxide samples at various experimental conditions.

In general, the XRD patterns show low intensity and relatively broad diffraction peaks. This might be due to the fact that the prepared materials are of very small size and tend to be amorphous. Figure 1a is the XRD pattern of titanium oxide sample prepared using hydrothermal method at 120 °C. The diffraction peaks at 2θ of 25.30°, 37.78°, 47.88°, 54.50° and 63.32° are ascribed to the crystallographic structure anatase phase (TiO_2, JCPDS card #84-1286). No other phases could be detected in the pattern. It is worth mentioning that the samples prepared at higher temperature (140 °C) gave a mixture phases. Figure 1b is the XRD pattern of the prepared sample using hydrothermal method at 100 °C. The XRD pattern exhibits diffraction peaks at 2θ of 25.43°, 27.51°, 30.76°, 36.10°, 37.82°, 48.00°, 54.30°, 63.04° and 69.13°, respectively. The presence of these diffraction peaks indicating that the deposited titanium dioxide pigment present in the form of mixed phases. The diffraction peaks can be assigned to mainly a mixture of anatase (TiO_2, JCPDS card #84-1286) and brookite phases (TiO_2, JCPDS card #72-0100) with the presence of traces of rutile phase (TiO_2, JCPDS card #75-1753). Figure 1c is the XRD pattern of the prepared sample using hydrolysis method. The XRD pattern exhibits diffraction peaks at 27.26°, 36.14°, 41.16°, 43.79°, 54.23°, 56.30°, 62.92° and 68.67°. All the diffraction peaks are assigned to rutile phase (TiO_2, JCPDS card #75-1753).

The crystallite size (d_{RX})for the prepared samples was determined by measuring the broadening of a most intense peak of the phase (main peak) in a diffraction pattern associated with a certain planar reflection within the crystal unit cell according to Debye–Scherrer equation as follows:

$$d_{RX} = k\lambda/\beta\cos\theta \quad (1)$$

where d_{RX} is the crystallite size, $k = 0.9$ is a correction factor account for particle shapes, β is the full width at half maximum (FWHM) of the most intense diffraction peak plane, λ is the wavelength of Cu target = 1.5406 Å, and θ is the Bragg's angle.

Here in the three XRD patterns for the three samples that prepared at different conditions, the diameters of the TiO_2 nanopigments are around 6.2, 11.7, and 9.9 nm for samples (a), (b) and (c), respectively.

The FT-IR spectra of the prepared TiO_2 nanopigments with different methods are given in Fig. 2. Many absorption bands belong to the organic functional groups such as OH and alkane (C_nH_n–) are detected. In anatase sample, a broad band in the range of 3,600–3,200 cm^{-1} is observed which related to stretching hydroxyl group (O–H), representing the presence of surface water as moisture. The other peak located at 1,635 cm^{-1} is for stretching of titanium carboxylate, which might be originated from TTIP precursor and ethanol. The presence of such peak might be due to incomplete washing process of the prepared powders. The bands between 800 and 450 cm^{-1} are assigned to the Ti–O stretching bands and give the characteristic absorption (transmittance) peak at around 500 cm^{-1} which is in excellent agreement with XRD results for rutile sample. Table 1 summarizes the results of FT-IR analysis.

Morphology

Figure 3 is the SEM micrographs of the deposited TiO_2 sample in the form of anatase. The sample was prepared via hydrothermal method at 120 °C. It is obvious that the sample has amorphous structure and it is mainly in the form of compact and nonporous structure.

TEM was used to further examine the particle size, crystallinity and morphology of samples. TEM bright field micrographs of anatase, mixture of anatase and brookite

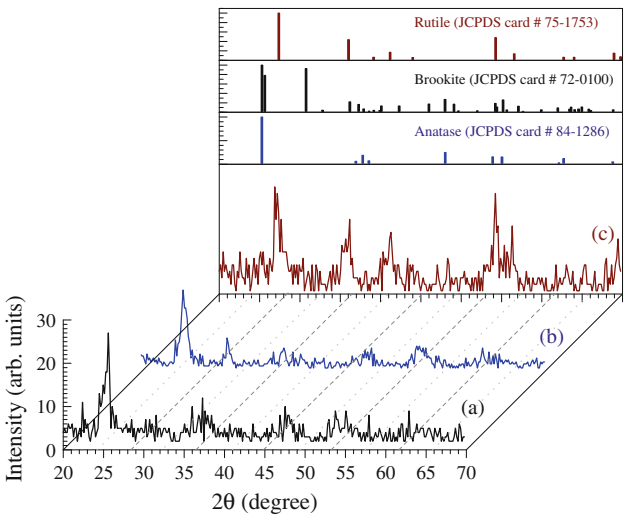

Fig. 1 X-ray diffraction patterns of TiO_2 nanopigment samples prepared by **a** hydrothermal method at 120 °C **b** hydrothermal method at 100 °C **c** hydrolysis method

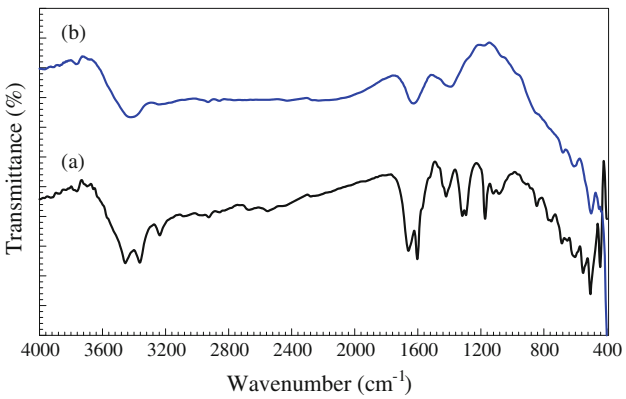

Fig. 2 FT-IR spectra of different TiO_2 nanopigments **a** anatase and **b** rutile samples

Table 1 FT-IR data obtained from analysis of TiO_2 nanopigments samples

S. no.	Peaks (cm^{-1})	Intensity (%)	Assignment	Phase	
				Anatase	Rutile
1	3,200, 3,363, 3,455 and 3,600	86.81, 82.22, 82.14 and 95	O–H	+	–
2	3,423	86.69	O–H	+	+
3	1,635	82.8	Titanium carboxylate	+	–
4	1,420	93.35	C–H	+	–
5	1,390	91.82	C–H	–	+
6	1,080	93.81	C–O	+	–
7	551, 602, 650, 685 and 800	80.47, 83.16, 86, 85.46 and 91.7	Ti–O	+	–
8	449, 500 and 678	71.25, 71 and 80.7	Ti–O	–	+

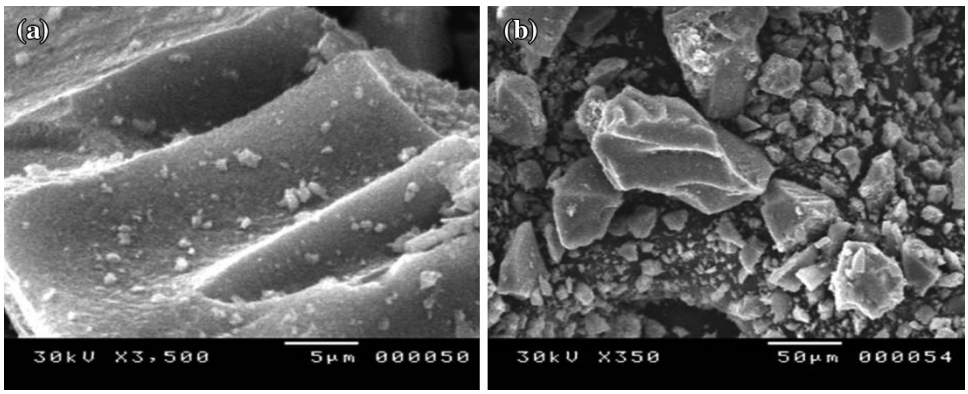

Fig. 3 SEM micrographs of prepared TiO_2 nanopigment sample (anatase) via hydrothermal method at 120 °C **a** high magnification **b** low magnification

and rutile are shown in Fig. 4. It is clearly seen that the TiO_2 nanopigments in anatase phase (Fig. 4a) are mostly of spherical-like morphology whereas in Fig. 4b TiO_2 nanopigments are consisting mainly of both rod and spherical-like structures. This result is in agreement with that obtained from XRD data where the sample is composed mainly of two mixed phases (anatase and brookite). The TiO_2 nanopigment in rutile phase, Fig. 4c, mostly has needle-like morphology.

Figure 5 shows the nitrogen adsorption–desorption curves of the prepared TiO_2 nanopigments. In general, the results reveal that the isotherms can be classified according to the IUPAC as reversible type IV. Type IV materials are characterized by mesoporosity with high energy of adsorption p/p°. It also shows hysteresis loop of type H1 where the two branches are almost vertical and nearly parallel indicated by the slit-shaped pores for anatase and rutile particles. This also implies the presence of regular even pores without interconnecting channels. The anatase manifested the highest BET surface area which amounted to 140.74 m^2/g, pore diameter amounted to 18.33 Å, and the total volume of pores was 0.237 cc/g. A lower BET specific surface area was demonstrated by rutile, which amounted to 60.621 m^2/g. A decrease in diameter and volume of pores could also be noted, which amounted to 14.669 Å and 0.122 cc/g, respectively.

UV–Vis and photoluminescence spectroscopy

Figure 6 shows the UV–visible absorption spectra of the TiO_2 nanopigments of the three prepared samples. The spectra reveal that the rutile sample shows the most narrow intensive peak at wavelength of 320 nm which is consistent with its known high refractive index and high brightness. In the case of anatase and brookite samples, the peak obtained at wavelength equal to 280 nm is broader than the other peak due to the appearance of the two phases as confirmed by XRD analysis. The anatase sample obtained less intensive peak than rutile peak at approximate wavelength of 300 nm. The band gap energies (Eg) of TiO_2 nanopigments were calculated using the equation:

$$E_g = hC/\lambda_{int} \quad (2)$$

where h is Planck's constant (4.135×10^{-6} eV nm); C, the velocity of light (3×10^8 ms^{-1}), and λ is the wavelength (in nm) corresponding to the intersection of extension of linear parts of the spectrum of y-axis and x-axis. From Fig. 6, the energy gaps for anatase, mixture of anatase and brookite and rutile are 3.36, 3.30 and 3.37 eV, respectively. Bulk titanium oxide has a band gap in the range of ~3 eV. For low dimensional nanostructured TiO_2 materials, electrons and holes are expecting to move shorter distances approximated by the indirect band gap

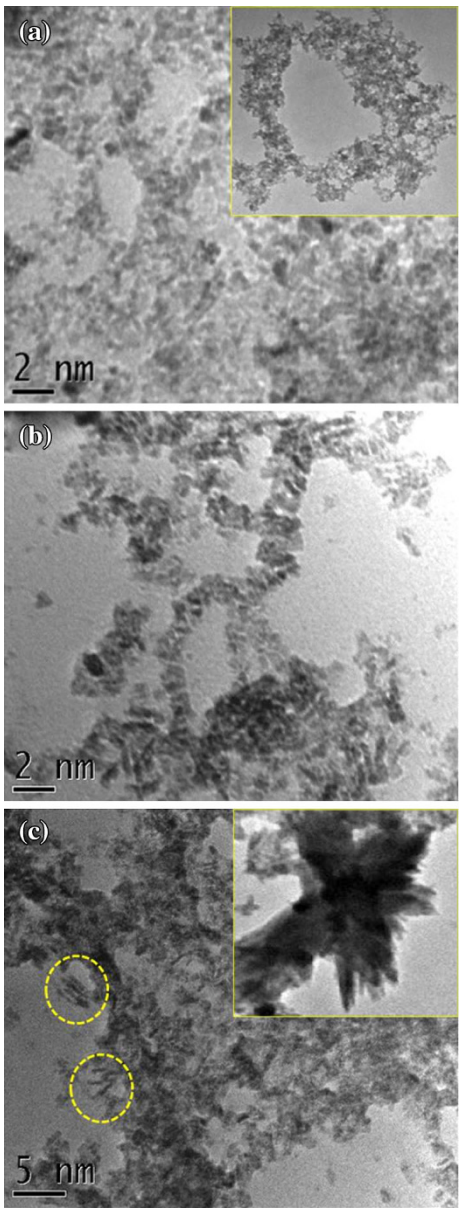

Fig. 4 TEM micrographs of TiO_2 nanoparticles of **a** anatase, **b** anatase + brookite **c** rutile phase structures. *Inset* in **a** represents general view of anatase spherical nanoparticles. *Inset* in **c** is a general view of rutile needle clusters. *Dotted circles* refer to individual single needle-like structures

between highest occupied and lowest unoccupied states. However, due to the large surface-to-volume ratio, lower dimensional TiO_2 nanostructures tend to have larger band gaps.

Figure 7 shows the PL spectra of TiO_2 nanopigments collected after an excitation at wavelength of 320 nm. As seen from the spectra, relatively broad bands at 358 nm and at 380 nm are detected for all samples. These emission bands are most probably originated from quantum confinement in nanocrystals.

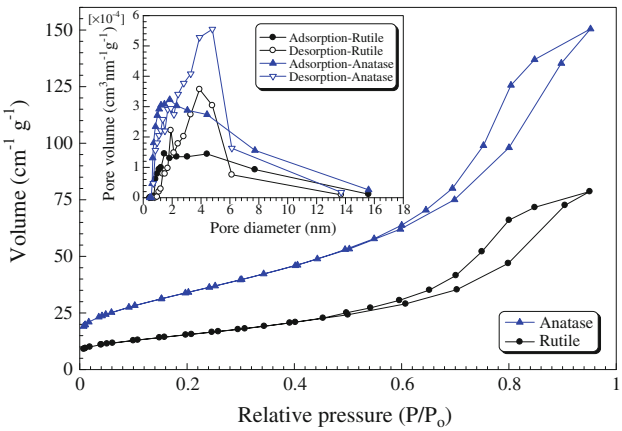

Fig. 5 N_2 adsorption–desorption isotherms and pore size distribution of the anatase and rutile prepared pigment

Application in paper coating

Optical properties

The optical properties of paper products are very important parameters, mostly due to their esthetic aspects; however, they also play an important role in print or writing showing through paper product. The properties are defined by reflecting ability, absorbing capacity and penetration of light through paper. Table 2 illustrates the effect of the prepared nano titanium dioxide phases in conjunction with clay on brightness and opacity of the prepared coated paper. It can be clearly seen that along with the increase in the amount of titanium dioxide in relation to clay, the paper ISO brightness and the opacity increased compared with pure clay-coated paper, because the inherent high light scattering coefficients of titanium dioxide pigment led to higher brightness and opacity as it limits the amount of light that can be transmitted through the paper. Comparing the three prepared nano titanium dioxide pigments, Table 2 shows that rutile pigment has the highest brightness value. This is in consistent with the results of UV–visible spectra in Fig. 6 which reveal that rutile pigment has the highest intensive peak. No significant difference in brightness appears upon changing the addition level of titanium dioxide from 30 to 50 % for sample rutile, a mixture (Anatase + Brookite) and anatase, respectively (Table 2). The opacity of the coated paper slightly increased upon using the prepared nano titanium dioxide pigments.

Physical properties

Table 2 summarized the data obtained for optical and physical properties of coated papers having the prepared nanopigments. It shows that an increase in the addition levels of nano titanium dioxide pigments leads to substantial decrease in coated paper roughness. When a coating mixture

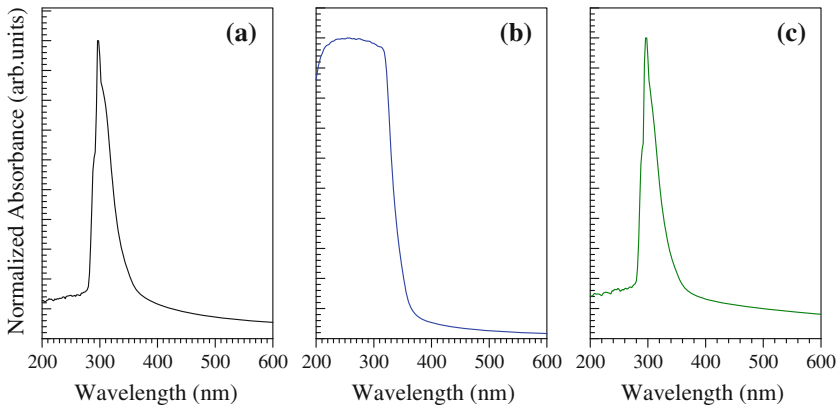

Fig. 6 UV–Vis absorption spectra of TiO_2 nanopigments. **a** Anatase, **b** mixture of brookite and anatase and **c** rutile samples

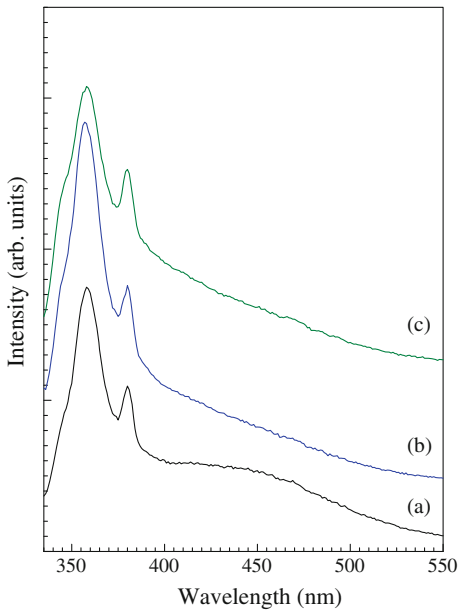

Fig. 7 Photoluminescence spectra of TiO_2 nanopigments. **a** Anatase, **b** anatase + brookite and **c** rutile samples. The samples are excited at wavelength of 320 nm

is applied to the paper, the dewatering or water penetration into the base paper induces the immobilization of the coating layer. The coating layer is further immobilized during the subsequent drying process, leading to shrinkage of the structure. When nano titanium pigment is incorporated in the coating mixture, the shrinkage of the coating layer during consolidation is counteracted. Apparently, this pigment act as spacers between the clay plates decreased the overall packing density (i.e., produce coated paper with loose packing), leading to high fiber coverage and a smooth surface of the coated paper (Gullichsen et al. 2000; Camilla et al. 1994). The same effect is shown for the three types of nano titanium dioxide pigments. The effect is more pronounced at 50 % additional level and greatest effect was obtained with rutile pigment, the percentage decrease reached to 40, 24 and 25 % for rutile, a mixture (Anatase + Brookite) and anatase, respectively.

The gloss of the clay-coated paper is much higher than the titanium dioxide-coated paper. This may be due to the disturbance of the platy structure of the clay upon the addition of TiO_2. Table 2 shows the air permeability's (porosities) of the coated papers for clay, and clay/nano TiO_2 systems. It is evident that blend of TiO_2 with clay with percent 70:30 has the lowest air permeance value. This may be due to the nanopigments fill in the narrow pores created between clay particles. As the percent of titanium pigments increased, the porosity significantly increased. In clay coating layer the particle integrity and void network extended uniformly throughout the entire coating. This void network is truly three-dimensional, interconnecting not just in the *Z* direction but in the machine and cross-machine directions as well. The high level of nano TiO_2 in clay

Table 2 Optical and physical properties of coated papers having the prepared nano TiO_2 pigments

Test	Clay	Rutile/clay additions		(Anatase + Brookite)/clay additions		Anatase/clay additions	
		70:30	50:50	70:30	50:50	70:30	50:50
Brightness (%)	92.60	92.73	93.15	92.07	92.38	92.70	92.97
Opacity (%)	96.47	96.90	97.13	96.51	96.83	96.74	97.01
Gloss (%)	14.58	7.84	9.29	8.61	9.69	8.34	10.79
Roughness (ml/min) before calendering	84.8	84	55.4	78.4	67.7	76.2	67.2
Roughness (ml/min) after calendering	80	65	48	71	61	69	60
Porosity (ml/min)	8.3	3.7	26.4	2.6	27.6	0.3	21.1

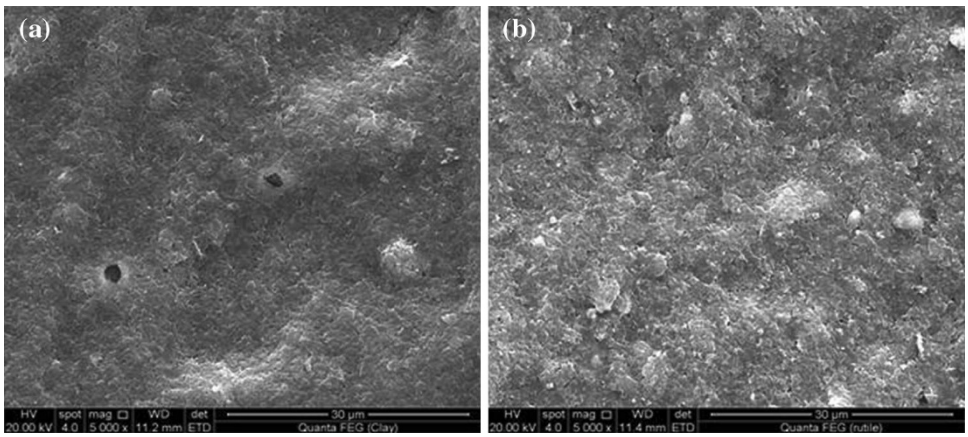

Fig. 8 SEM micrographs of **a** clay and **b** clay/rutile coated paper at 50 % additions

coating mixture disturbs the high packing characteristic of clay pigment providing a loose coating layer packing consequently, imparting more air flow pathway.

Surface structures

Figure 8 is the electron micrographs of paper coated with clay-based pigment (a) and clay/rutile nano TiO_2 (b) (at 50 % addition level). Figure 8 shows that the coating layer follows the tangent of the underlying fibers giving an open and rough surface. Some recesses and vallies are appeared. Upon addition of nano TiO_2, smooth and homogeneous coated paper surfaces have been obtained, this can explain the lower roughness of this coated paper sample.

Conclusions

Pure crystallographic anatase and rutile TiO_2 phase samples have been successfully prepared by hydrothermal at 120 °C and hydrolysis methods, respectively. The application of the prepared nanopigments in paper coating reveals that a small amount of TiO_2 is sufficient to achieve significant gains in brightness and opacity, because of the high light scatter ability of the pigment and the refractive index contrast with the other materials in coated paper composite. Also imparting nano TiO_2 pigment into coating formula significantly decreases the surface roughness. The optimal proportion to enhance the porosity of the paper is 70:30 % nano TiO_2 pigment to clay additions.

References

Bok Y, Sig M, Duck E, Gyu H, Young W, Hee S, Lee G, Park S, Hong S (2007) Hydrothermal synthesis of titanium dioxides from peroxotitanate solution using different amine group-containing organics and their photocatalytic activity. Catal Today 124:88–93

Camilla R, Eriksson U, Rigdah M (1994) Consolidation behavior and gloss of paper coatings based on plastic pigments. Nord Pulp Pap Res J 9:254

Dahlvik P, Lohmander S, Lason L, Rigdahl M (2000) Relations between the rheological properties of coating colour and their performance in pilot-scale coating. Nord Pulp Pap Res J 15:106

Deorsola FA, Vallauri D (2008) Synthesis of TiO_2 nanoparticles through Gel Combustion process. J Mater Sci 43:3274–3278

Fumin W, Zhansheng S, Feng G, Motonarib A (2007) Morphology control of anatase TiO2 by surfactant-assisted hydrothermal method. China J Chem Eng 15:754–759

Gullichsen J, Paulapuro H, Lehtinen E (2000) Papermaking science and technology. Fapet/Tappi Series, part 11

Inagaki M, Nakazawa Y, Hirano M, Kobayashi Y, Toyoda M (2001) Preparation of stable anatase-type TiO_2 and its photocatalytic performance. Inter J Inorg Mater 3:809–811

Jiaguo Y, Jimmy Y, Bei C, Xiujian Z (2003) Preparation and characterization of highly photoactive nanocrystalline TiO_2 powders by solvent evaporation induced crystallization method. Sci in China 46(6) series B

John MC (2006) Chemistry of TiO_2 nanoparticles. Puplished PhD thesis, Proquest

Jun W, Gang Z, Zhaohong Z, Xiangdong Z, Guan Z, Teng M, Yuefeng J, Peng Z, Ying L (2007) Relations between the rheological properties of coating colour and their performance in pilot-scale coating. Dyes Pigm 75:335–343

Kobayashi M, Tomita K, Petrykin V, Yoshimura M, Kakihana M (2008) Direct synthesis of brookite-type titanium oxide by hydrothermal method using water-soluble titanium complexes. J Mater Sci 43:2158–2162

Kumar S, Sahoo T, Mohapatra M, Anand S, Yu Y (2009) Polyol-assisted synthesis of TiO_2 nano particles in a semi-aqueous solvent. J Phys Chem Solids 70:147–152

Mahshid S, Askari M, Sasani M (2007) Synthesis of TiO_2 nanoparticles by hydrolysis and peptization of titanium isopropoxide solution. J Mater Process Tech 189:296–300

Murray H, Elzea J (2005) Engineered clay products for the paper industry. Appl Clay Sci 29:199–206

Ninness BJ, Bousfield DW, Tripp CP (2003) Formation of a thin TiO_2 layer on the surfaces of silica and kaolin pigments through atomic layer deposition. A: Physicochem Eng Aspect 214:195–204

Qiong H, Xianming W, Peihua M, Xiaochuan D, Wuha UJ (2008) Alkali induced morphology and property improvements of tio_2 by hydrothermal treatment. J Wuhan Univ Tech Mater Sci Ed 23:503–506

Smook GA (1997) Handbook for pulp and paper technologists, 2nd edn. Angus Wilde Publications Inc., Bellingham

Wang H, Liu P, Cheng X, Shui A, Zeng L (2008) Effect of surfactants on synthesis of TiO_2 nano-particles by homogeneous precipitation method. Powder Tech 188:52–54

Yamamoto K, Tomita K, Fujita K, Kobayashi M, Petrykin V, Kakihana M (2009) Synthesis of TiO_2 using glycolatotitanium complex and post-synthetic hydrothermal crystal growth of TiO_2. J Cryst Growth 311:619–622

Zhang S, Liu C, Liu Y, Zhang Z, Mao L (2009) Room temperature synthesis of nearly monodisperserodlike rutile TiO_2 nanocrystals. Mater Lett 63:127–129